KIAS

New Physics in toponium's shadow?

The 16th Particle Physics Phenomenology Workshop (PPP16)

Jinheung Kim

KIAS

2026/06/16

Outline

1. Introduction

1.1 Quarkonium in Particle Physics

- Charmonium $(c\bar{c})$
  - In Nov. 1974, two experimental groups at BNL and SLAC independently discovered the J/ψ [1,2]
  - Evidence for the GIM mechanism, asymptotic freedom, and the quark model
- Bottomonium $(b\bar{b})$
  - The Υ was discovered at Fermilab in 1977 [3]
  - Discovery of the third-generation quark and the CKM matrix
- Toponium $(t\bar{t})$
  - Discovered at LHC in 2025 [4,5]

BNL

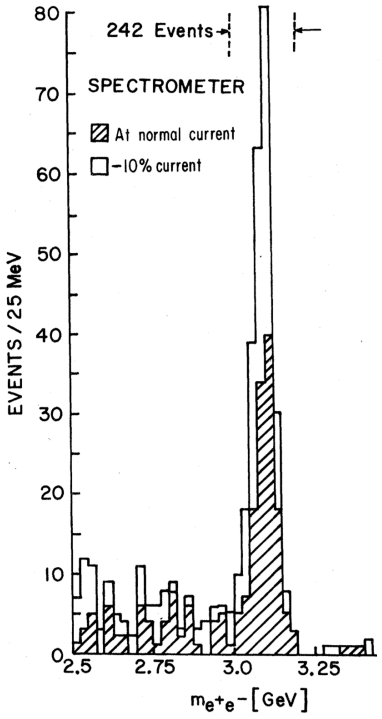

SLAC

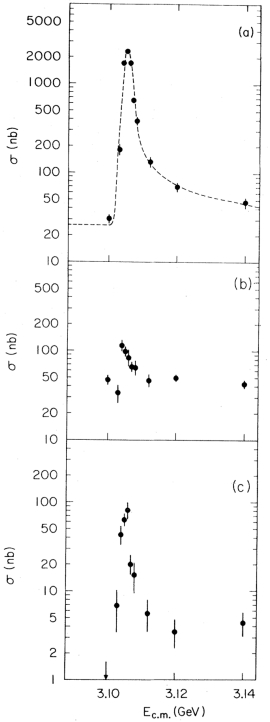

Fermilab

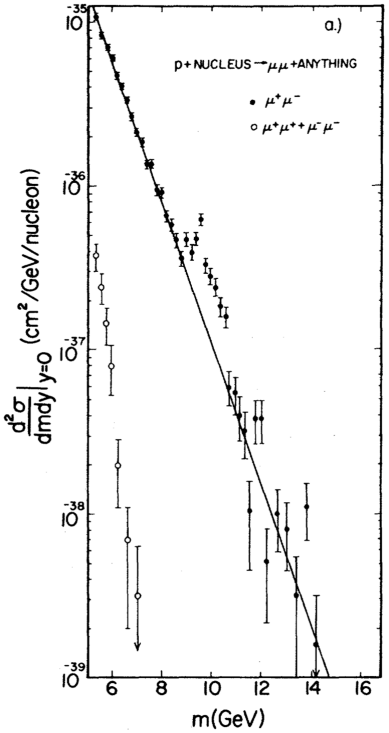

J/Ψ Υ

1.2 Toponium

$C_F = 4/3$

- Conceptually, toponium is the bound state of $t\bar{t}$.
- Near threshold, the system is approximately Coulombic, with reduced mass $m_t/2$, coupling strength $C_F\alpha_s$, and potential $V = -\frac{C_F\alpha_s}{r}$.
- This gives the typical scales: Bohr radius $a = (C_F\alpha_s m_t/2)^{-1}$ and velocity $v \sim C_F\alpha_s$.
- The formation time is $t_{\text{form}} \sim \frac{a}{v} \sim \frac{1}{m_t(C_F\alpha_s)^2} \sim (8\ \text{GeV})^{-1}$.
- The dominant decay channel of toponium is through top-quark decay, $T \to bWt$, with decay width $\Gamma \approx 2\Gamma_t$ [6]. Annihilation channels have branching ratios below 10^{-3} [7].
- The top-quark lifetime is $t_{\text{dec}} \sim \frac{1}{2\Gamma_t} \approx (2.6\ \text{GeV})^{-1}$.
- Since $t_{\text{dec}} \sim t_{\text{form}}$, the system decays before a stable bound orbit forms.
- Therefore, toponium appears as a quasi-bound state rather than a true bound state.

1.2 Toponium

- The nth S-wave energy level is given by $E_n = -\frac{C_F^2 \alpha_s^2 m_t}{4n^2} \approx -\frac{2\ \text{GeV}}{n^2}$.
- The energy differences between adjacent levels are smaller than the toponium width.
- As a result, the would-be toponium resonances overlap and cannot be resolved.
- Instead of narrow resonances, only a broad enhancement in the $t\bar{t}$ production cross section near threshold is expected at hadron colliders.

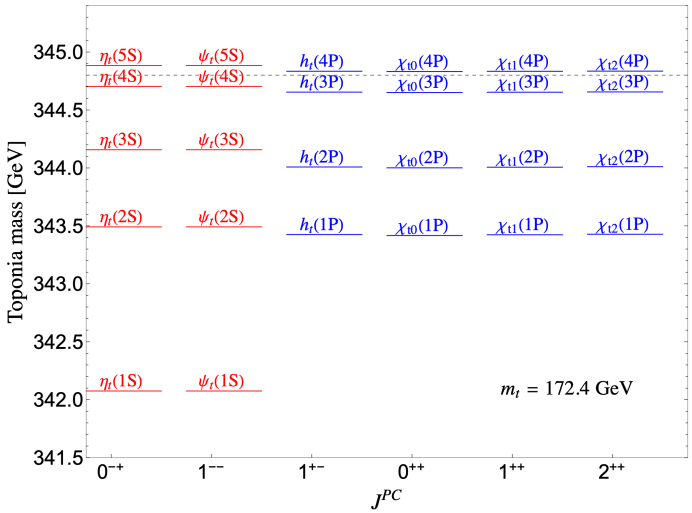

Figure 1: toponium energy levels [7]

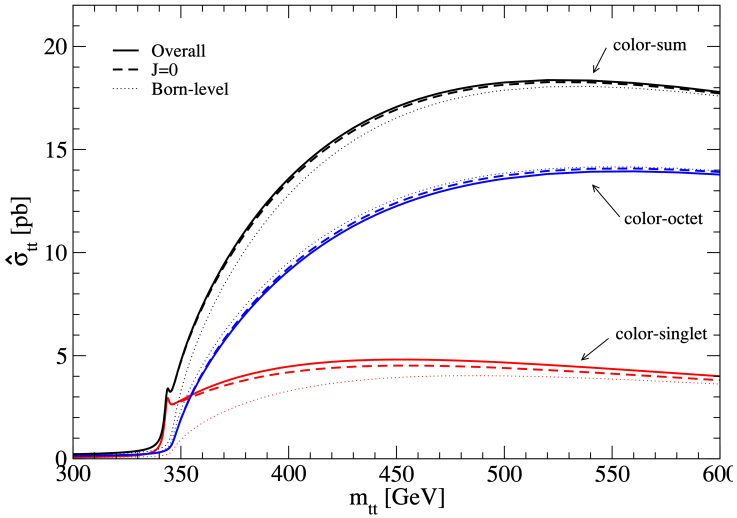

Figure 2: $t\bar{t}$ production cross section [8]

1.3 Why is toponium important?

- Verification of non-relativistic QCD
- Threshold physics in $t\bar{t}$ production
  - Entanglement [9,10], Top-quark mass [11,12], Top Yukawa coupling measurement [13,14], Top-quark width, CP properties, color structure, ...

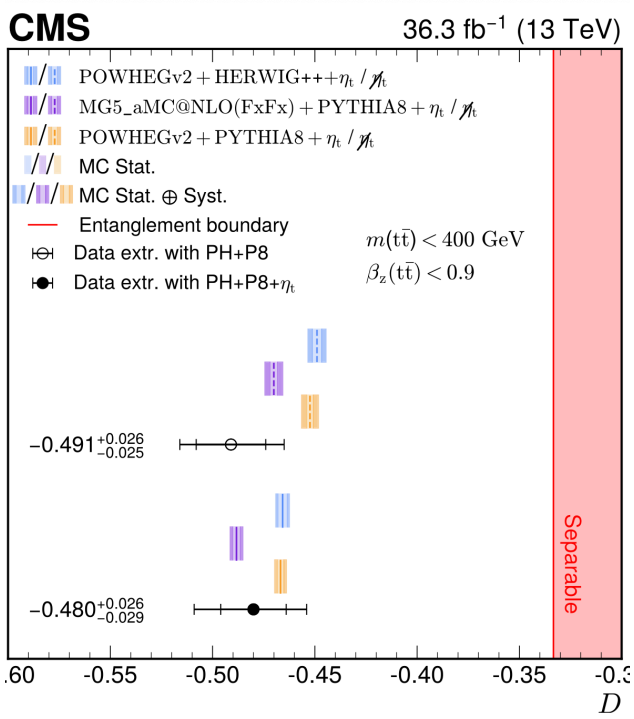

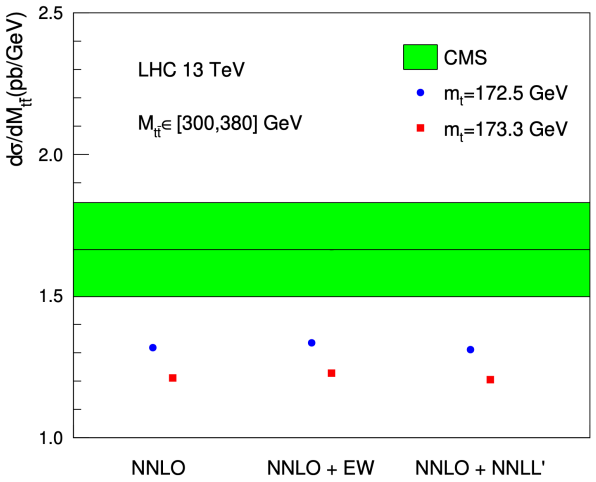

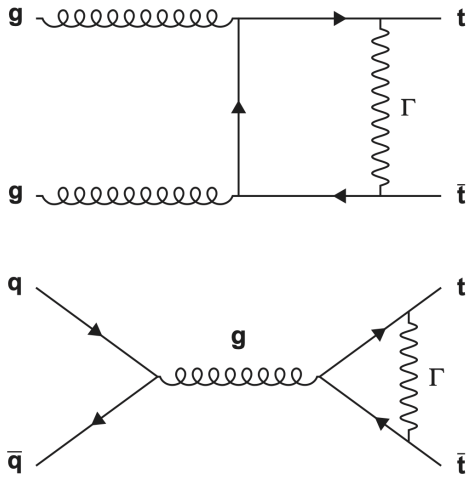

2. Calculation of toponium production rate

2.1 Calculation of toponium production rate

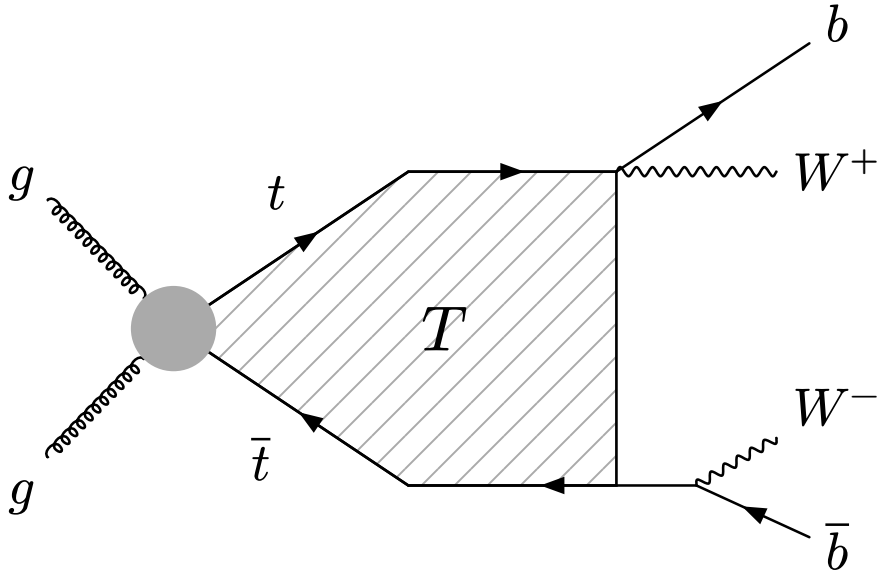

- Near the $t\bar{t}$ threshold, the top-quark velocity is small ($\beta = \sqrt{1 - \frac{4m_t^2}{\hat{s}}} \sim 0$).
- In this regime, Coulomb gluon exchanges $\left(\frac{\alpha_s}{\beta}\right)$ are enhanced, so ladder diagrams with multiple gluon exchanges are not suppressed. [15,16]
- Therefore, fixed-order perturbation theory breaks down, and a non-relativistic treatment is needed.

2.1 Calculation of toponium production rate

- The production amplitude can be factorized into a short-distance part and a long-distance part. [8,17,18]

$$\mathcal{M}\left(pp \to t\bar{t} \to bW^+\bar{b}W^-\right) = \mathcal{M}\left(pp \to t\bar{t} \to bW^+\bar{b}W^-\right)_{\text{tree}} \times \frac{G(E+i\Gamma_t, p)}{G_0(E+i\Gamma_t, p)},$$

- G_0 is the free Green's function, given by $\frac{1}{E+i\Gamma-p^2/m_t}$
- The non-relativistic Green's functions $G(E,p)$ are defined by

$$\left[E + i\Gamma_t - \left\{-\frac{\nabla^2}{m_t} + V^{(1)}_{\text{QCD}}(r)\right\}\right]\tilde{G}(E+i\Gamma_t, r) = \delta^3(r)$$

$$G(E+i\Gamma_t, p) = \int d^3r e^{-ipr}\tilde{G}(E+i\Gamma_t, r)$$

- where $E = m_{t\bar{t}} - 2m_t$ is the binding energy, p is the three-momentum of the t in the $t\bar{t}$ rest frame, and Γ_t is the top-quark width.

2.2 Calculation of toponium production rate

$$V_{\text{coul}} = -C_F \alpha_S / r$$

- $G(E + i\Gamma; p)$ is obtained by solving the Lippmann-Schwinger equation:

$$G(E + i\Gamma; p) = G_0(E + i\Gamma; p) + G_0(E + i\Gamma, p) \int \frac{\mathrm{d}^3 q}{(2\pi)^3} V_{\text{coul}}(p - q) G(E + i\Gamma; q)$$

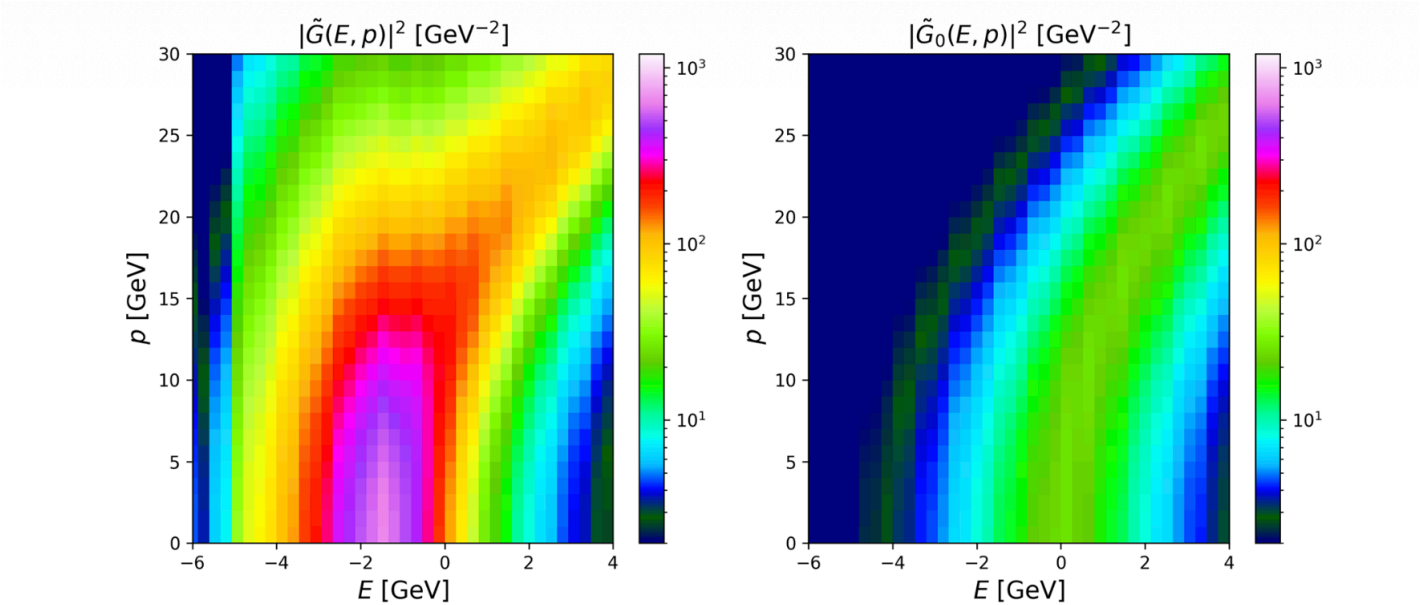

Figure 3: The non-relativistic Green's function $G(E, p)$ [19]

2.3 Production in collider

- In the threshold region ($\beta \sim 0$), the S-wave ($L = 0$) contribution to the cross section is dominant. Contributions from the P-wave ($L = 1$) are suppressed by β^2 [20].
- e^+e^- collider
  - $t\bar{t}$ is produced mainly via γ/Z (vector current).
  - Near threshold, spin-1 ($S = 1$) $t\bar{t}$ states dominate.
- Hadron collider
  - $gg \to t\bar{t}$
    - Depending on the helicity combination, $J = 0, 2, \ldots$
    - In the near-threshold region, the $J = 0$ state is dominant.
    - Near threshold, spin-0 ($S = 0$) states dominate.
  - $q\bar{q} \to t\bar{t}$
    - Mainly produces the $J = 1$ state.
    - Spin-1 states dominate.

2.4 Simulation toponium at the LHC

- E: binding energy
- p: momentum of t in the $t\bar{t}$ rest frame

- How to simulate toponium signals in MC simulations?

Toy model [21]

$$\mathcal{L} \supset -\frac{1}{4} g_{gg\eta_t} \phi_{\eta_t} G_{\mu\nu} \tilde{G}^{\mu\nu} - i g_{tt\eta_t} \phi_{\eta_t} \bar{t} \gamma^5 t$$

- Easy to implement
- Limited accuracy

Reweight method [19]

$$|\mathcal{M}|^2 \to |\mathcal{M}|^2 \left| \frac{G(E;p)}{G_0(E;p)} \right|^2$$

- More accurate
- Difficult to implement

- How to implement the reweighting method in event generators (MG5)?
  - Modify `matrix1_orig.f`
  - Modify the color matrix from $\begin{pmatrix} 16 & -2 \\ -2 & 16 \end{pmatrix}$ to $\begin{pmatrix} 2 & 2 \\ 2 & 2 \end{pmatrix}$
  - Find E and p in the $t\bar{t}$ rest frame and obtain the value of G/G_0
  - Apply the reweighting: `MATRIX1 = MATRIX1*DCONJG(GREEN)*GREEN`
  - Recently, `PYTHIA8`(v8.137) has implemented a similar approach to the reweighting method [22].

3. Excess at the LHC and its interpretation

3.1 CMS and ATLAS analysis

More Detail

- CMS and ATLAS collaborations have reported an excess in the $t\bar{t}$ invariant-mass spectrum near threshold.
  - CMS: $\sigma(\eta_t) = 8.8^{+1.2}_{-1.4}$ pb [4], single lepton: 5.1 ± 0.9 pb[23]
  - ATLAS: $\sigma(\text{NRQCD}) = 9.3^{+1.4}_{-1.3}$ pb [5]
- Di lepton channel: $t\bar{t} \to bW^+\bar{b}W^- \to b\bar{b}\ell^+\nu\ell^-\bar{\nu}$
- Event selection
  - OS, $N_\ell = 2$, $N_j \geq 2$, $N_b \geq 1$.
  - $\vec{p}_{\nu(\bar{\nu})}$ calculated by analytic method.

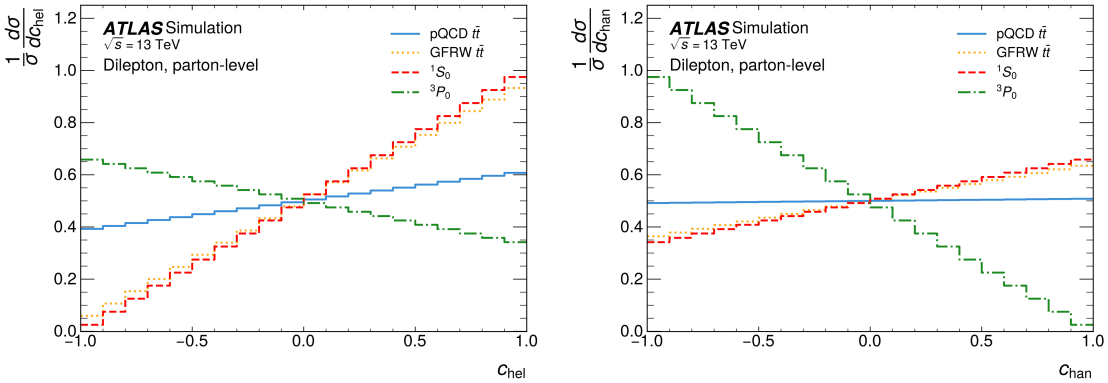

(a) (b)

- Spin correlation variables, c_{han}, c_{hel}.
  - c_{han}: $\widehat{\ell^+} \cdot \widehat{\ell^-}$, $\widehat{\ell^\pm}$ is the unit vector of the momenta of $\ell^\pm$ in the rest frames of their parent $t(\bar{t})$.
  - c_{hel}: similarly but with a sign flip of the t quark direction component.

3.1 CMS and ATLAS analysis

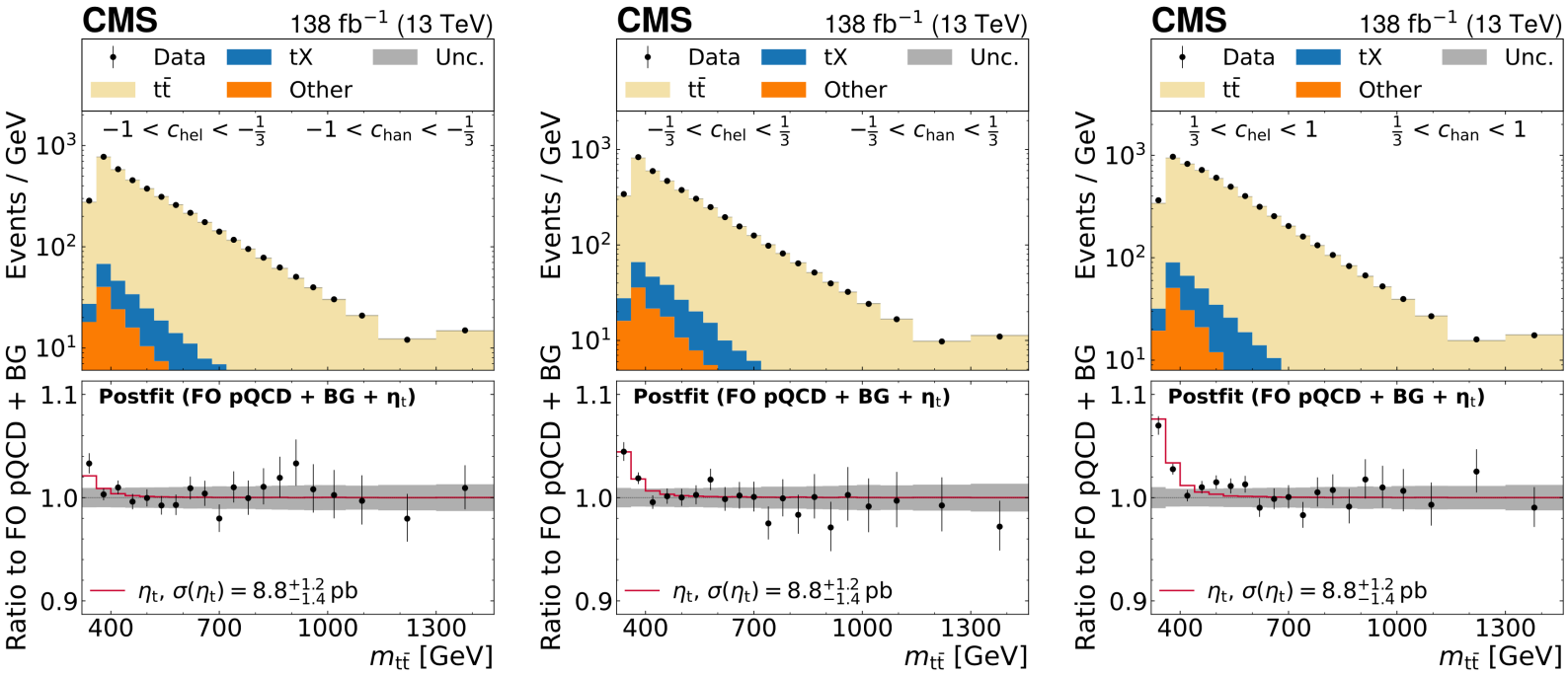

Figure 5: The excess reported by CMS [4].

3.1 CMS and ATLAS analysis

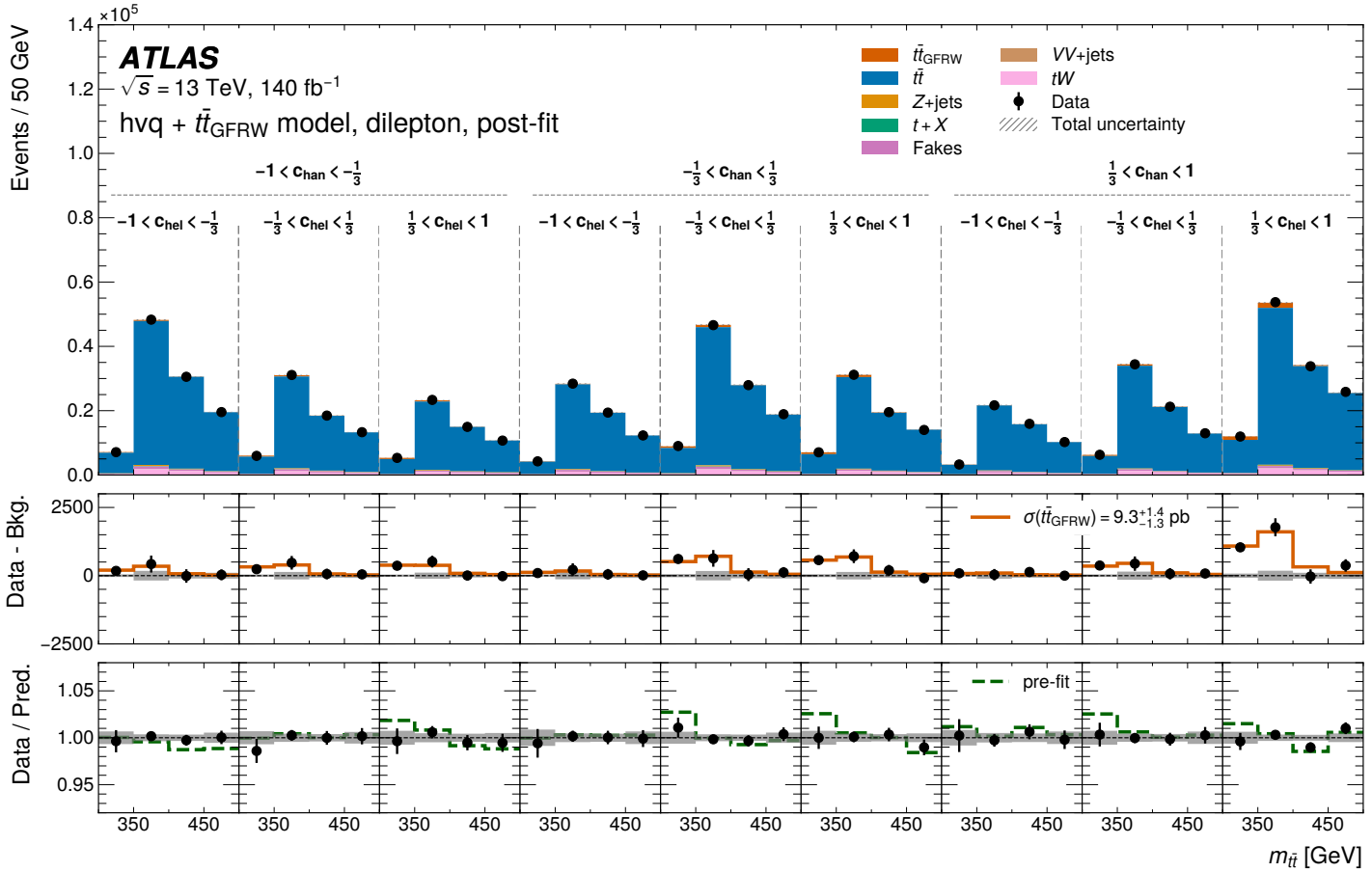

Figure 6: The excess reported by ATLAS [5].

3.2 BSM Scenario

- Can the excess be explained by BSM effects alone? Yes.

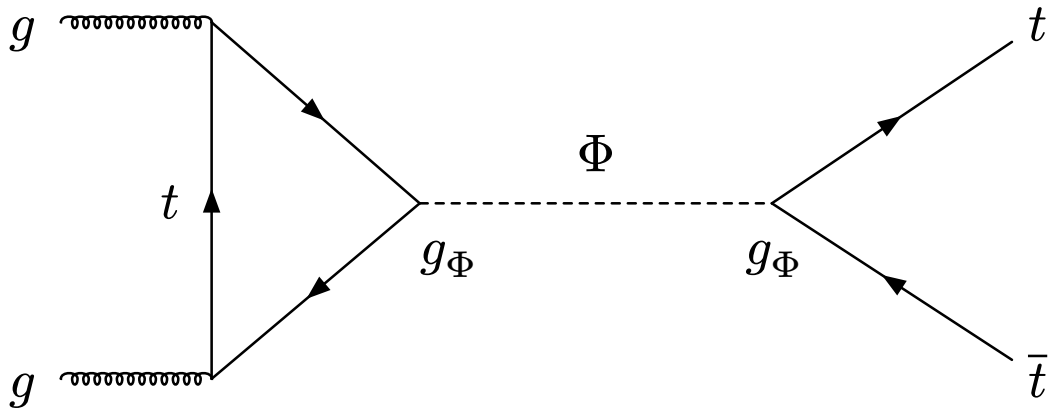

Figure 7: Feynman diagrams for BSM pseudoscalar A

- CMS reports the best-fit points for $\Phi = H/A$ without η_t included in the background [24]
  - $M_A = 365$ GeV, $\frac{\Gamma}{M} = 2\%$, $g_A = 0.77 \pm 0.04$
  - $M_H = 365$ GeV, $\frac{\Gamma}{M} = 2\%$, $g_H = 0.96^{+0.16}_{-0.25}$
  - $-2\Delta \ln L \approx 53$, indicating a strong preference for the CP-odd scenario.

3.2 BSM Scenario

- *Lu et al.* [25]
  - 2HDM
  - $M_A = 365$ GeV, $t_\beta = 1.28 \pm 0.128$, $s_{\beta-\alpha} = 1$
  - Theoretical constraints: $600\ \text{GeV} \lesssim M_H, M_{H^\pm} \lesssim 720\ \text{GeV}$
  - A large $\sigma(gg \to H)\text{Br}(H \to ZA)$ is excluded by ATLAS $Zt\bar{t}$ data [26]
  - The conventional 2HDM cannot explain the excess. Other extensions of the 2HDM are needed.

- *Djouadi et al.* [27]
  - How to distinguish the excess from A or toponium?
  - Interference between A and SM QCD amplitudes
  - Other production channels:
    - $gg \to hA \approx 25$ fb
    - $gg \to t\bar{t}A \approx 15$ fb

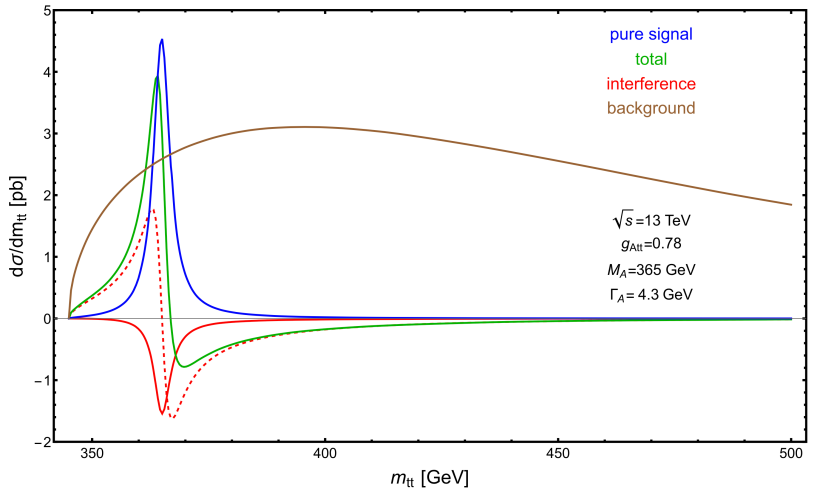

4. New physics in toponium's shadow?

Thomas Flacke, Benjamin Fuks, Dongchan Kim, JK, Seung J. Lee
2512.03220, accepted to PLB

4.1 Motivation

- CMS provides limits on the BSM parameter space with and without toponium in the background [24]

$$\mathcal{L}_A \supset i g_A \frac{m_t}{v} \bar{t} \gamma_5 t A, \quad \mathcal{L}_H \supset i g_H \frac{m_t}{v} \bar{t} t H$$

- The measured signal strengths are
  - without toponium background:
    - $g_A = 0.77 \pm 0.04$, $g_H = 0.96^{+0.16}_{-0.25}$
  - with toponium background:
    - $g_A = 0.35^{+0.28}_{-0.35}$, $g_H = 0.75^{+0.26}_{-0.49}$
- In the presence of new physics, the toponium production rate may be modified.
- When setting limits on the BSM parameter space, changes in the toponium production rate should be taken into account.

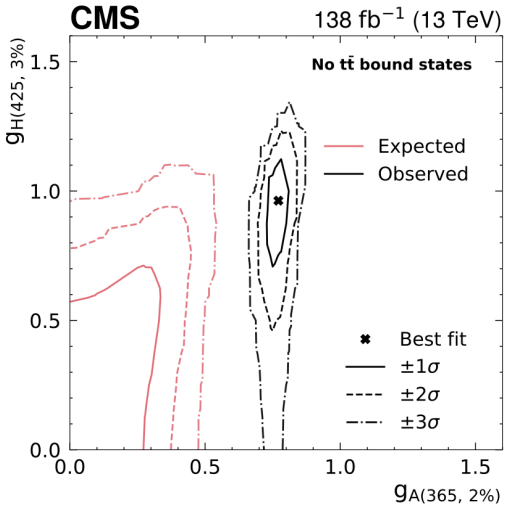

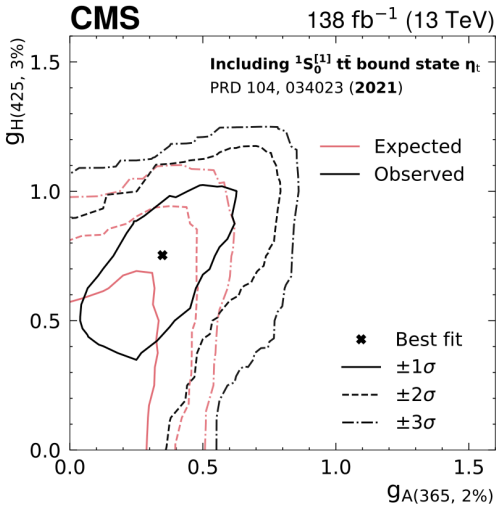

4.2 Model

- We consider the simple model which includes a pseudoscalar particle a that couples to top quark and gluon.

$$\mathcal{L} \supset \frac{1}{2}\partial_\mu a \partial^\mu a - \frac{1}{2}M_a^2 a^2 + \frac{\alpha_s}{8\pi v}\tilde{\kappa}_g G^a_{\mu\nu} G^{a,\mu\nu} + 2c_t a \bar{t} i\gamma_5 t, \quad \tilde{\kappa}_g = \kappa_g + \kappa_t$$

- κ_g arises from the UV theory (e.g., a composite Higgs model).
- $\kappa_t = \frac{v c_t}{2m_t} A^A_{1/2}\left(\frac{M_a^2}{4m_t^2}\right)$ is an effective coupling induced by the top-quark loop.
- $A^A_{1/2}$: form factor
  - $A^A_{1/2} = 2\tau^{-1} f(\tau)$
  - $f(\tau) = \begin{cases} \arcsin^2\sqrt{\tau} & \text{for } \tau \leq 1 \\ -\frac{1}{4}\left[\ln\left(\frac{1+\sqrt{1-\tau^{-1}}}{1-\sqrt{1-\tau^{-1}}}\right) - i\pi\right]^2 & \text{for } \tau > 1 \end{cases}$

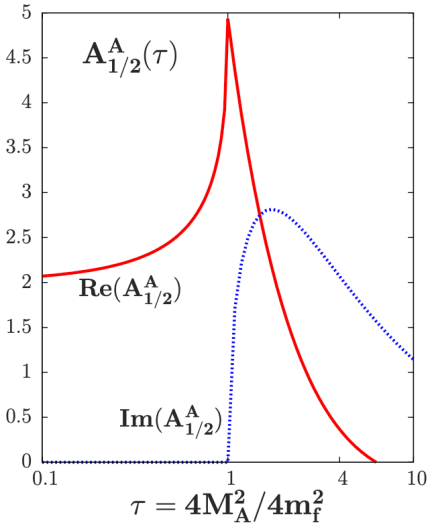

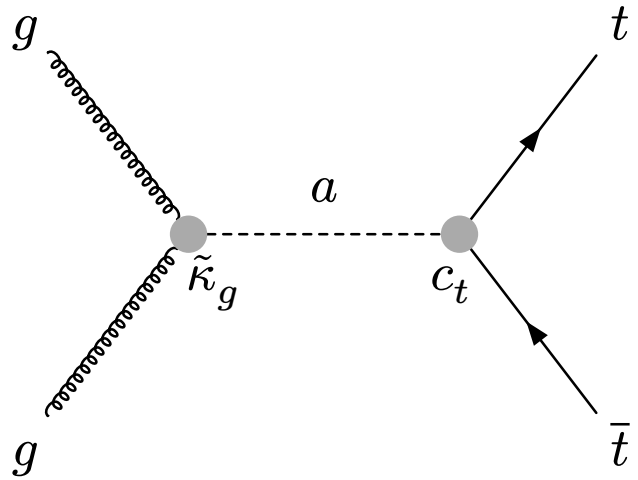

4.3 Method

- We consider the four-body decay process $gg \to t\bar{t} \to bW^+\bar{b}W^-$.
- In the presence of BSM contributions, the toponium production rate is modified as follows:

$$\left|\mathcal{M}\left(gg \to t\bar{t} \to bW^+\bar{b}W^-\right)\right|^2_{\text{BSM}} \to \left|\mathcal{M}\left(gg \to t\bar{t} \to bW^+\bar{b}W^-\right)\right|^2_{\text{BSM}} \left|\frac{G(E;p)}{G_0(E;p)}\right|^2$$

- The attraction force from new pseudoscalar is suppressed by $e^{-M_a r}$. We only consider the QCD contributions, so the same $G(E;p)$ is not changed.
- Since only the color-singlet $t\bar{t}$ state can form a bound state, we project onto the color-singlet configuration by modifying the color matrix.

$$\begin{pmatrix} 16 & -2 & 6 \\ -2 & 16 & 6 \\ 6 & 6 & 18 \end{pmatrix} \to \begin{pmatrix} 2 & 2 & 6 \\ 2 & 2 & 6 \\ 6 & 6 & 18 \end{pmatrix}.$$

4.3 Method

- The reweighting is restricted to the near-threshold region, $m_{t\bar{t}} < 350$ GeV and $p < 50$ GeV, where the non-relativistic approximation is valid.
- To simplify the analysis, we treat M_a and c_t as free parameters and fix $\frac{\Gamma}{M_a}$ to 1% or 5%. κ_g is adjusted to reproduce the chosen Γ.

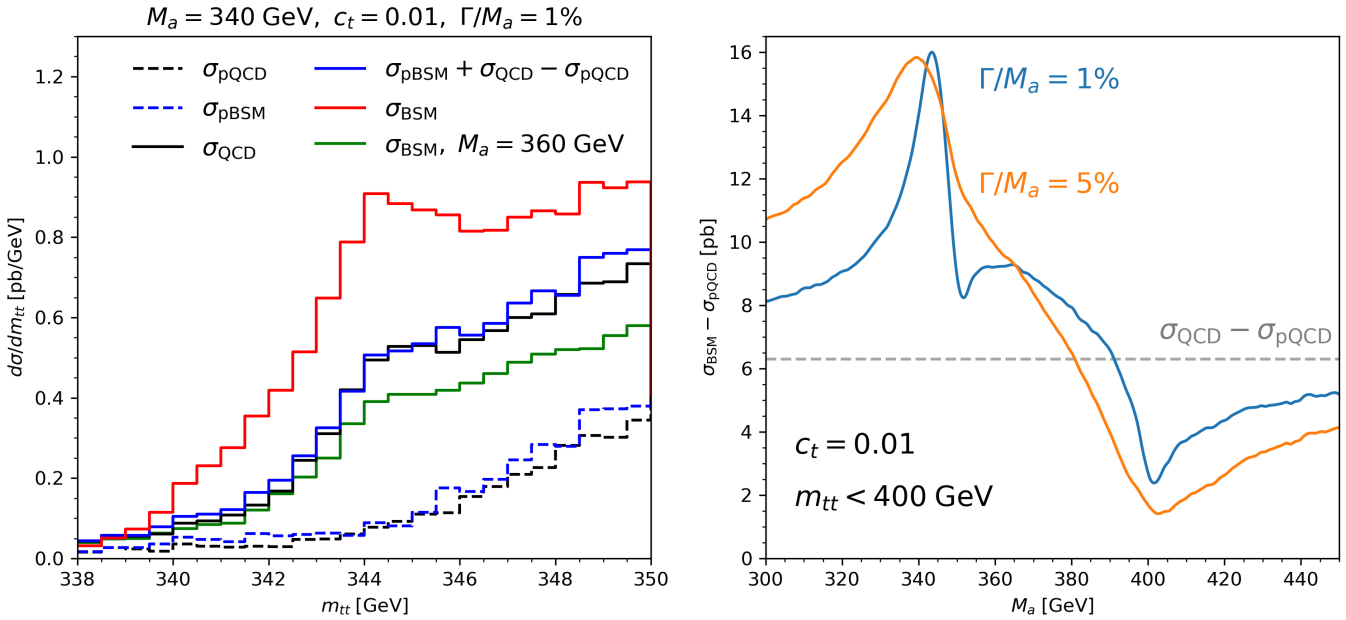

4.4 Result

- The observed cross section is $\sigma_{\text{obs}} = 9.0 \pm 1.3$ pb [28].
- The SM prediction for the toponium production rate is $\sigma_{\text{SM}} = 6.43$ pb [21]
- The excess is localized in the low-mass region, $m_{t\bar{t}} < 400$ GeV, suggesting a possible threshold-related origin.
- For $m_{t\bar{t}} > 400$ GeV, the BSM contribution is constrained to satisfy $\sigma_{\text{BSM}} < 1.05\sigma_{\text{pQCD}}$, indicating that new physics effects must remain small away from threshold.
- We define $\Delta\sigma = \sigma - \sigma_{\text{pQCD}}$ to quantify deviations from the pQCD prediction.

4.4 Result

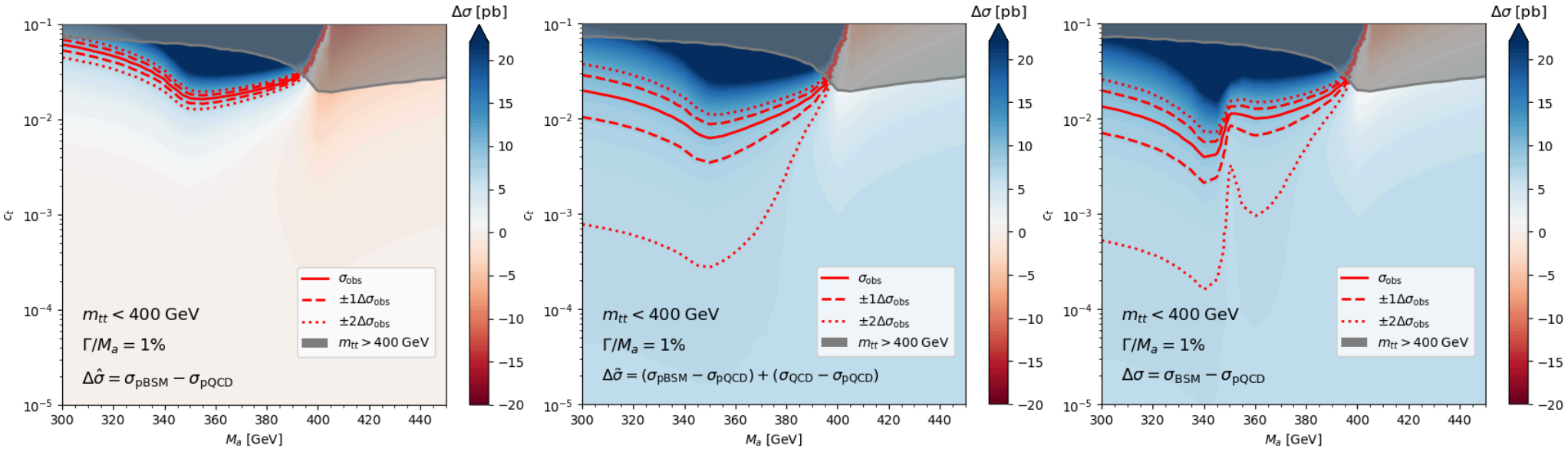

Figure 12: Allowed parameter space for $\Gamma/M_a = 1\%$, without toponium (left), with SM toponium (mid), with BSM toponium (right)

4.4 Result

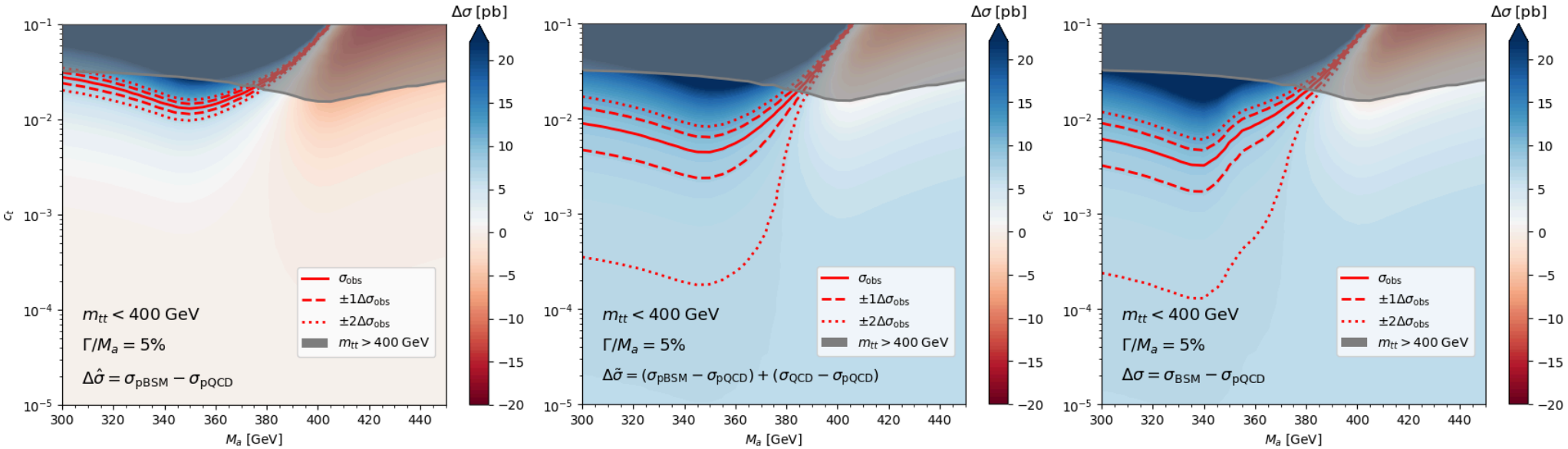

Figure 13: Allowed parameter space for $\Gamma/M_a = 5\%$

5. Conclusion

5.1 Conclusion

Summary

- A toponium signal near the $t\bar{t}$ threshold provides direct access to non-relativistic QCD dynamics, and the excess reported by CMS and ATLAS is consistent with it.
- The toponium production rate can be consistently computed by matrix-element reweighting with the non-relativistic Green's functions — and the same machinery extends naturally to new physics.
- In the presence of BSM interactions, sizable interference with SM QCD can significantly modify the threshold production rate. Toponium and new physics cannot be treated as independent components.
- Consequently, limits on the BSM parameter space can change, particularly in the region $M_a \approx 2m_t$.

5.1 Conclusion

Open questions for us to pursue

- **Discrimination:** What observable can cleanly separate a toponium signal from a BSM pseudoscalar — spin correlations, entanglement, or the interference line shape?
- **Theory precision:** How large is the uncertainty on the SM toponium rate, and can we push the Green's-function calculation to higher order?
- **Consistent interference:** How do we treat the BSM–toponium interference beyond the near-threshold approximation and match it to fixed-order QCD?
- **Complementary channels:** Can $t\bar{t}h$, four-top, or the single-lepton channel break the toponium / new-physics degeneracy?
- **Future colliders:** What would a lepton-collider threshold scan add to pin down the threshold dynamics?

6. Backup

6.1 Details of CMS and ATLAS analysis

Back

6.1.1 CMS analysis [4]

- CMS analysis $\sigma(\eta_t) = 8.8^{+1.2}_{-1.4}$ pb
  - Event selection
    - OS $N_\ell = 2$, $p_T^{\ell(\text{lead,sub})} > 25(20)$ GeV, $m_{\ell\ell} > 20$ GeV
    - SF: $p_T^{\text{miss}} > 40$ GeV, $|m_{\ell\ell} - 91\ \text{GeV}| > 15$ GeV
    - $N_j \geq 2$, $N_b \geq 1$, $p_T^j > 30$ GeV, $p_T^b > 20$ GeV
  - Event reconstruction
    - all b-tagged jets in the event as $b\left(\overline{b}\right)$ candidates.
    - $N_b = 1$: one non-b-tagged jet $\rightarrow b\left(\overline{b}\right)$ candidate.
    - Maximizing the likelihood of $m_{\ell^+ b}$ and $m_{\ell^- \overline{b}}$
  - Neutrino momentum reconstruction
    - Analytic method [29].
    - For multiple solutions, smallest $m_{t\bar{t}}$ selected.
    - Repeat 100 times with smearing momenta of the $\ell^+, \ell^-, b, \overline{b}$.
    - Final result of the reconstruction is taken as the weighted averages.
    - Resolution: 15% at the $t\bar{t}$ threshold, 25% for higher $m_{t\bar{t}}$

6.1 Details of CMS and ATLAS analysis

Back

6.1.2 ATLAS analysis [5]

- ATLAS analysis: $\sigma(\text{NRQCD}) = 9.3^{+1.4}_{-1.3}$ pb
  - Event selection
    - OS $N_\ell = 2$, $p_T^{\text{lead}} > 25/27/28$ GeV for data taken in 2015,2016, and 2017+18.
    - SF: $m_{\ell\ell} > 15$ GeV, 81 GeV $< m_{\ell\ell} < 101$ GeV, $p_T^{\text{miss}} \geq 60$ GeV
    - $N_j \geq 2$, $N_b \geq 1$, $p_T^j > 25$ GeV, $m_{t\bar{t}} \leq 500$ GeV
  - Event reconstruction
    - $N_b \geq 2$, leading and subleading b-tagged jets are taken as $b\left(\bar{b}\right)$ candidates.
    - $N_b = 1$, the leading non-b-tagged jet is taken as $b\left(\bar{b}\right)$ candidate.
  - Neutrino momentum reconstruction
    - Ellipse Method [30]
    - For multiple solutions, smallest $m_{t\bar{t}}$ selected.
    - If no solution is found, repeated with different masses $m_t \sim \mathcal{N}(172.5, 1.48)$, $m_W \sim \mathcal{N}(80.379, 2.085)$; the lowest $m_{t\bar{t}}$ is chosen.
    - Resolution: 22% at the $t\bar{t}$ threshold, 18% for $m_{t\bar{t}} \approx 500$ GeV

6.1 Details of CMS and ATLAS analysis

6.1.3 CMS H/A analysis

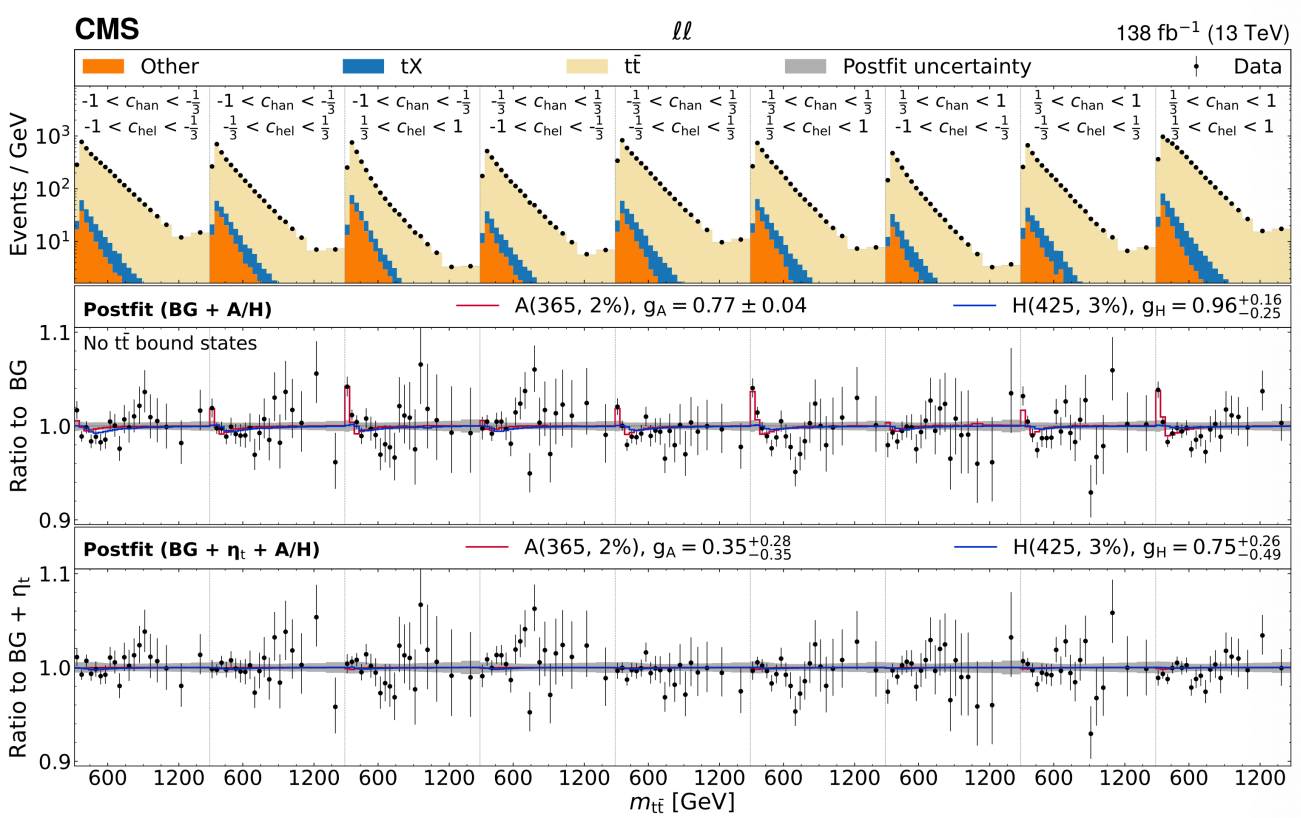

Figure 14: The explanation of the excess by BSM pseudoscalar particle [24]

6.2 Detail analysis of Lu

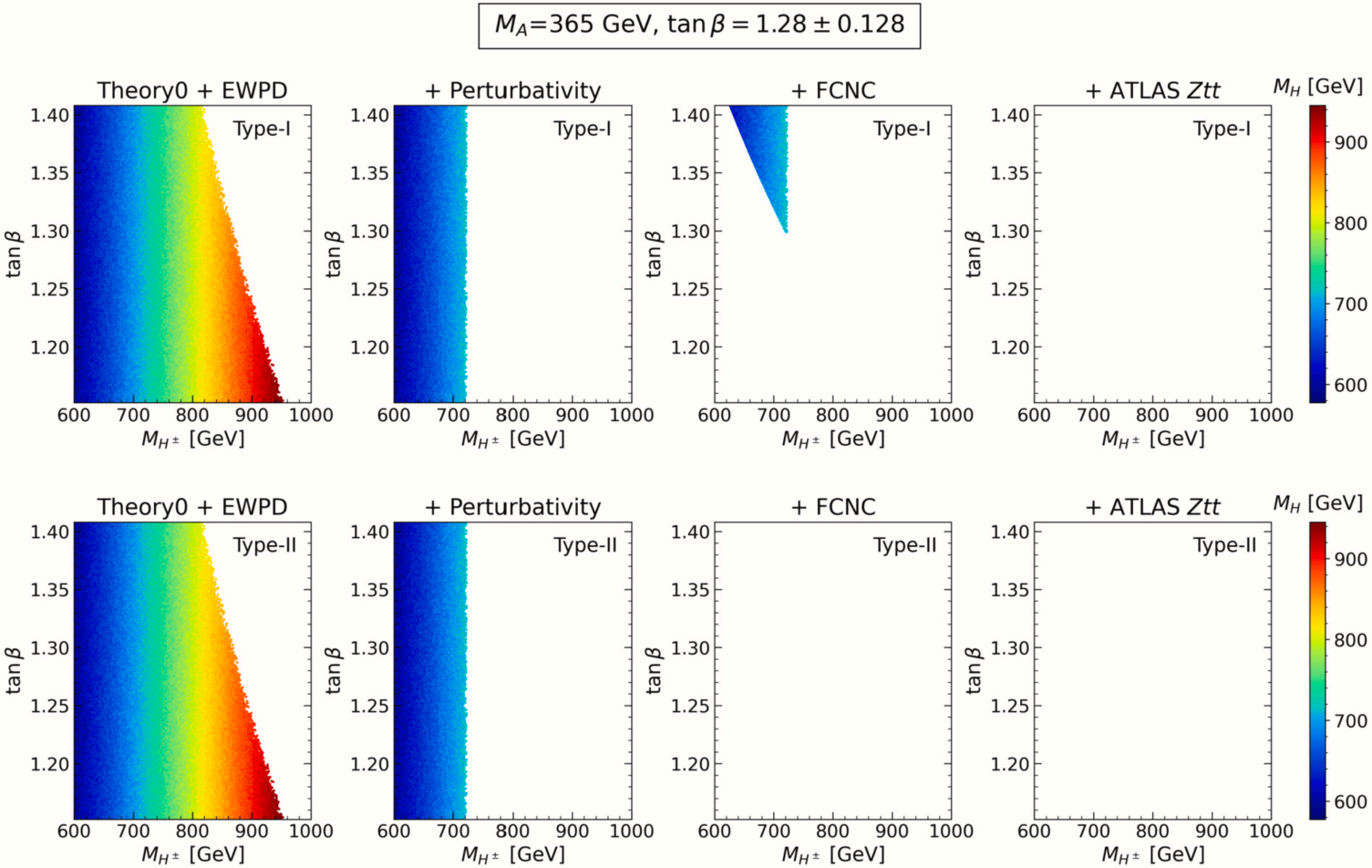

Figure 15: Parameter scanning result in 2HDM [25]

References

[1] J. J. Aubert and others, Experimental Observation of a Heavy Particle J, Phys. Rev. Lett. **33**, 1404 (1974).

[2] J. E. Augustin and others, Discovery of a Narrow Resonance in e^+e^- Annihilation, Phys. Rev. Lett. **33**, 1406 (1974).

[3] S. W. Herb and others, Observation of a Dimuon Resonance at 9.5 GeV in 400 GeV Proton-Nucleus Collisions, Phys. Rev. Lett. **39**, 252 (1977).

[4] A. Hayrapetyan and others, Observation of a pseudoscalar excess at the top quark pair production threshold, Rept. Prog. Phys. **88**, 87801 (2025).

[5] G. Aad and others, Observation of a cross-section enhancement near the t\bar{t} production threshold in \sqrt{s}=13 TeV pp collisions with the ATLAS detector, (2026).

[6] J. H. Kuhn and P. M. Zerwas, The Toponium Scenario, Phys. Rept. **167**, 321 (1988).

[7] Y. Bai, T.-K. Chen, and Y. Yang, Toponia at the HL-LHC, CEPC, and FCC-ee, (2025).

[8] Y. Sumino and H. Yokoya, Bound-state effects on kinematical distributions of top quarks at hadron colliders, JHEP **9**, 34 (2010).

[9] A. Hayrapetyan and others, Observation of quantum entanglement in top quark pair production in proton–proton collisions at \sqrt{s} = 13 TeV, Rept. Prog. Phys. **87**, 117801 (2024).

[10] G. Aad and others, Observation of quantum entanglement with top quarks at the ATLAS detector, Nature **633**, 542 (2024).

[11] W.-L. Ju, G. Wang, X. Wang, X. Xu, Y. Xu, and L. L. Yang, Top quark pair production near threshold: single/double distributions and mass determination, JHEP **6**, 158 (2020).

[12] M. V. Garzelli, J. Mazzitelli, S. O. Moch, and O. Zenaiev, Top-quark pole mass extraction at NNLO accuracy, from total, single- and double-differential cross sections for t\overline{t} + X production at the LHC, JHEP **5**, 321 (2024).

[13] A. M. Sirunyan and others, Measurement of the top quark Yukawa coupling from \mathrm{t\bar{t}} kinematic distributions in the lepton+jets final state in proton-proton collisions at \sqrt{s} = 13 TeV, Phys. Rev. D **100**, 72007 (2019).

[14] G. Aad and others, Measurement of the top-quark Yukawa coupling from t\overline{t} production in the lepton+jets final state using pp collisions at \sqrt{s}=13 TeV with the ATLAS detector, JHEP **1**, 117 (2026).

[15] M. J. Strassler and M. E. Peskin, The Heavy top quark threshold: QCD and the Higgs, Phys. Rev. D **43**, 1500 (1991).

[16] Y. Sumino, Review on physics of e^{+} e^{-} \to t \bar{t} near threshold, Acta Phys. Polon. B **25**, 1837 (1994).

[17] Y. Sumino, K. Fujii, K. Hagiwara, H. Murayama, and C. K. Ng, Top quark pair production near threshold, Phys. Rev. D **47**, 56 (1993).

[18] M. Jezabek, J. H. Kuhn, and T. Teubner, Momentum distributions in t anti-t production and decay near threshold, Z. Phys. C **56**, 653 (1992).

[19] B. Fuks, K. Hagiwara, K. Ma, and Y.-J. Zheng, Simulating toponium formation signals at the LHC, Eur. Phys. J. C **85**, 157 (2025).

[20] K. Hagiwara, Y. Sumino, and H. Yokoya, Bound-state Effects on Top Quark Production at Hadron Colliders, Phys. Lett. B **666**, 71 (2008).

[21] B. Fuks, K. Hagiwara, K. Ma, and Y.-J. Zheng, Signatures of toponium formation in LHC run 2 data, Phys. Rev. D **104**, 34023 (2021).

[22] T. Sjöstrand, V. A. Khoze, and C. T. Preuss, Top Pair Threshold Revisited, (2026).

[23] Observation of a pseudoscalar excess at the top quark pair production threshold in the single lepton channel, (2026).

[24] A. Hayrapetyan and others, Search for heavy pseudoscalar and scalar bosons decaying to a top quark pair in proton–proton collisions at \sqrt{s} = 13\,\textrm{TeV}, Rept. Prog. Phys. **88**, 127801 (2025).

[25] C.-T. Lu, K. Cheung, D. Kim, S. Lee, and J. Song, Can a pseudoscalar with a mass of 365 GeV in two-Higgs-doublet models explain the CMS tt\textasciimacron excess?, Phys. Lett. B **859**, 139121 (2024).

[26] Search for a CP-odd Higgs boson decaying to a heavy CP-even Higgs boson and a Z boson in the \ell\ell t\bar{t} and \nu\bar{\nu}b\bar{b} final states using 140 fb^{-1} of data collected with the ATLAS detector, (2023).

[27] A. Djouadi, J. Ellis, and J. Quevillon, Contrasting pseudoscalar Higgs and toponium states at the LHC and beyond, Phys. Lett. B **866**, 139583 (2025).

[28] Observation of a cross-section enhancement near the t\bar{t} production threshold in \sqrt{s} =13 TeV pp collisions with the ATLAS detector, (2025).

[29] L. Sonnenschein, Analytical solution of ttbar dilepton equations, Phys. Rev. D **73**, 54015 (2006).

[30] B. A. Betchart, R. Demina, and A. Harel, Analytic solutions for neutrino momenta in decay of top quarks, Nucl. Instrum. Meth. A **736**, 169 (2014).